A phenomonological calculation of the effect of external magnetic fields on the Morin transition in hematite
by Robert William Gable

A thesis submitted to the Graduate Faculty in partial fulfillment of the requirements for the degree of MASTER OF SCIENCE in Electrical Engineering
Montana State University


Abstract:
The effect of applied magnetic fields on the Morin transition of hematite (α-Fe2O3) has been investigated from a phenomenological point of view; all applied fields are directed in the (lll) plane. The calculation shows a temperature depression that is nearly proportional to the square of the applied field and a transition temperature which is close to the experimentally observed results.

Using a dipolar model only, the effect of certain impurities on the Morin transition has also been investigated and found to be inconsistent with experiment.

1028-21

# A PHENOMONOLOGICAL CALCULATION OF THE EFFECT OF EXTERNAL MAGNETIC FIELDS ON THE MORIN TRANSITION IN HEMATITE

by

ROBERT WILLIAM GABLE

A thesis submitted to the Graduate Faculty in partial fulfillment of the requirements for the degree

of

MASTER OF SCIENCE

in

Electrical Engineering

Approved:

Head, Major Department

Chairman, Examining Committee

Graduate Dean

MONTANA STATE UNIVERSITY
Bozeman, Montana

December, 1968

ACKNOWLEDGMENT

I would especially like to recognize the following people for their help while writing and assembling this paper: Dr. John P. Hanton for serving as thesis advisor and providing informative discussion on the topic, Mr. Calvin Ransom who provided the experimental data, and Mrs. Rosemary Hoyer who typed the original manuscript.

TABLE OF CONTENTS

# LIST OF TABLES

# LIST OF FIGURES

ABSTRACT

The effect of applied magnetic fields on the Morin transition of hematite ($\alpha$-$Fe_2O_3$) has been investigated from a phenomonological point of view; all applied fields are directed in the (111) plane. The calculation shows a temperature depression that is nearly proportional to the square of the applied field and a transition temperature which is close to the experimentally observed results.

Using a dipolar model only, the effect of certain impurities on the Morin transition has also been investigated and found to be inconsistent with experiment.

# CHAPTER I

# INTRODUCTION

In recent years a considerable amount of research has been devoted to studying the curious magnetic properties of hematite ($\alpha$-$Fe_2O_3$) single crystals. The emphasis has been particularly intense since the discovery of neutron diffraction spectroscopy which is suitable to the investigation of antiferromagnetic materials. In fact, neutron diffraction methods produced the first experimental verification of Néel's original theory of antiferromagnetism.[1] He assumed the material was composed of two sublattices with equal magnetizations that are arranged in an antiparallel fashion, each sublattice being strongly coupled ferromagnetically within itself.

Hematite is the iron member of a group of antiferromagnetic sesquioxides all of which are isomophous with corundum, $\alpha$-$Al_2O_3$. The most common are the oxides of Cr, Fe, Ti, and V. The respective antiferromagnetic structures differ only by lattice parameters and spin arrangement. In each case, the oxides have a trigonal unit cell containing four magnetic cations. For $\alpha$-$Fe_2O_3$ the spins are directed in a +--+ order along the triaxial or c axis [111] as in Fig. 1a. The arrangement of the unit cells is such that all spins within any triaxial plane (111) are parallel, and adjacent planes contain oppositely directed spins as shown in Fig. 1b.

Since the actual distribution of spin states of any magnetic material is determined by a Boltzmann factor, it is evident that magnetic quantities will be strongly temperature dependent. The temperature dependency of the magnetic properties of hematite is particularly interesting and unique among the sesquioxides.

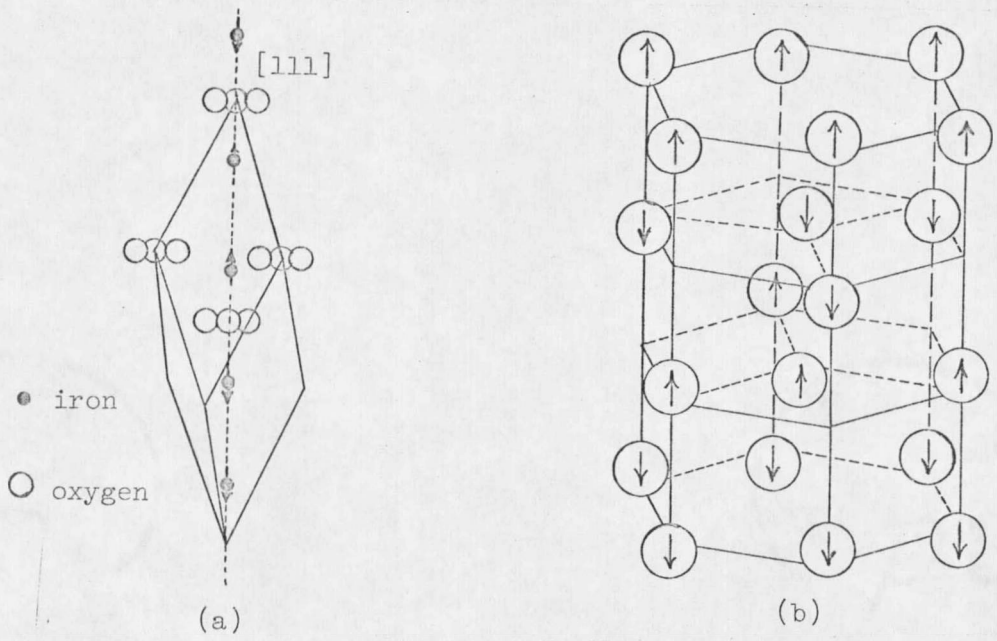


Fig. 1. (a) Trigonal cell of $\alpha$-$Fe_2O_3$ showing spin arrangement of cation spin, (b) planar arrangement Fe ions.

For temperatures below a certain critical value, for the moment defined as $T_m$, the material is a pure antiferromagnet with spins aligned collinear with the c axis. In this antiferromagnetic phase, the magnetic susceptibilities $\chi_{\parallel}$ and $\chi_{\perp}$, for external fields applied parallel and perpendicular to the c axis respectively, behave according to the standard molecular field theory.

At the temperature $T_m$, about 260°K for pure hematite, there is a second-order phase transition and the spins rotate 90° into the triaxial plane (111) in such a manner that antiferromagnetism is still retained.* The effect of this rotation causes $\chi_{\parallel}$ to rise abruptly to the $\chi_{\perp}$ value,

*The actual situation is one of weak ferromagnetism. This will be explained later.

since the spin direction is now perpendicular to the c axis. On the other hand, $\chi_\perp$ would ideally stay constant since the spins are nearly free to rotate in the triaxial plane. The critical temperature, $T_m$, is often referred to as the Morin transition temperature after F. J. Morin[2] who originally reported the effect.

The cause of this phase transition has been the subject of discussion from the time of its discovery. One phenomenological approach to the effect shows that the spin-flip may be interpreted as a change of sign of the first-order crystalline anisotropy constant.[3,4] This is consistent with the definition, to first-order, of a uniaxial anisotropy energy of the form:

$$F = (K/2) \sin^2\alpha, \qquad 1.1$$

where $\alpha$ is the angle between the magnetic moment and the trigonal axis and K is the first-order anisotropy constant. The thermodynamic free energy, due to anisotropy, is then a minimum when $\alpha=0$ for $K>0$ and when $\alpha=\frac{\pi}{2}$ for $K<0$. From this idea, a phenomenological interpretation can be made by assuming that if the anisotropy constant is positive, the preferred or easy direction of the magnetic moment is collinear with the trigonal axis. Above $T_m$, however, the sign of K is negative and the spins lie in the triaxial plane.

The temperature range between $T_m$ and the Néel temperature is complicated by an additional effect which is of interest. All of the spins are perpendicular to the c axis; but they are not directly antiparallel. Due to an anisotropic spin coupling the magnetic moments tend to be canted at a small angle with respect to each other. This results in a weak ferromagnetism since there is a net magnetic moment in the plane. The situation is

pictured in Fig. 2. The weak ferromagnetism of hematite and other compounds has been investigated thermodynamically by I. Dzyaloshinski[5] using magnetic symmetry arguments and quantum mechanically by T. Moriya.[6]

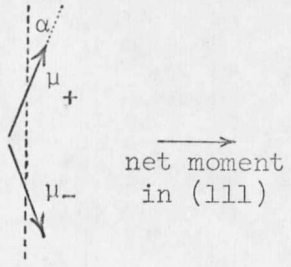


Fig. 2. Weak ferromagnetic arrangement of magnetic moments in the triaxial plane.

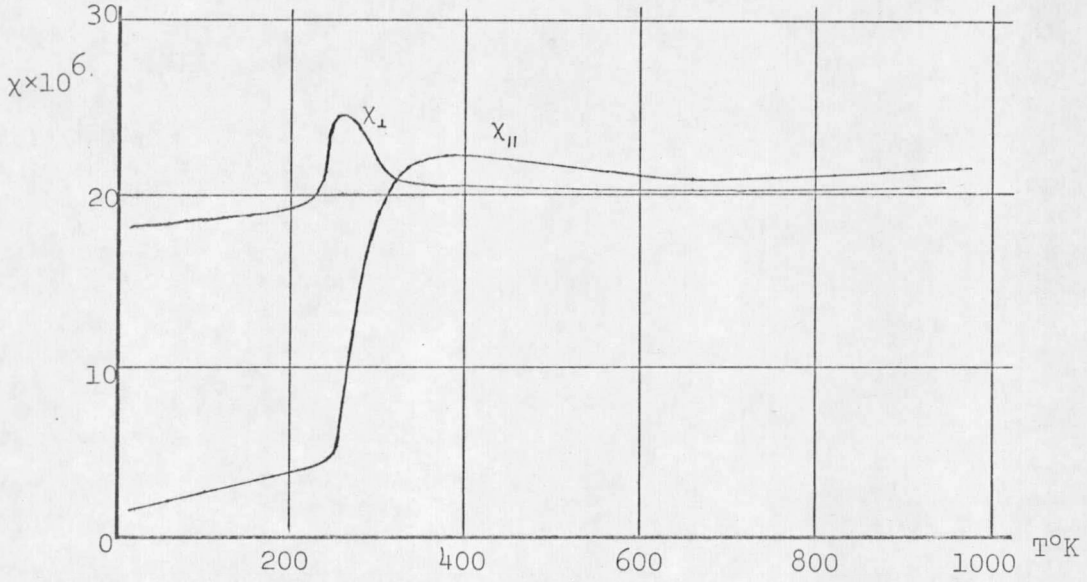


Fig. 3. Parallel and perpendicular susceptibility as a function of temperature for a natural hematite crystal.

As mentioned earlier, the perpendicular susceptibility is only ideally a constant through the Morin transition. Since the spin-flip is also a transition to weak ferromagnetism, there is actually a hump in $\chi_\perp$ at the Morin temperature. Fig. 3 shows $\chi_\parallel$ and $\chi_\perp$ vs. temperature as measured by L. Néel and R. Pauthenet.[7]

The main portion of the work to be presented here will be concerned with an effect which occurs when external magnetic fields are applied in the basal plane. In addition to the induced magnetization from $\chi_{\perp}$, there is a noticable decrease in the Morin temperature with increasing fields. The magnitude of the temperature shift is approximately -0.5 to -1.0°C/Koe.

The experimental data in Fig. 4 was taken on a vibrating sample magnetometer at MSU by Mr. Calvin Ransom. The plotted quantities are sample magnetization vs. temperature with the external field as the parameter. The plot clearly shows the depression of $T_m$ by the external field and the transition to weak-ferromagnetism for temperatures above $T_m$.

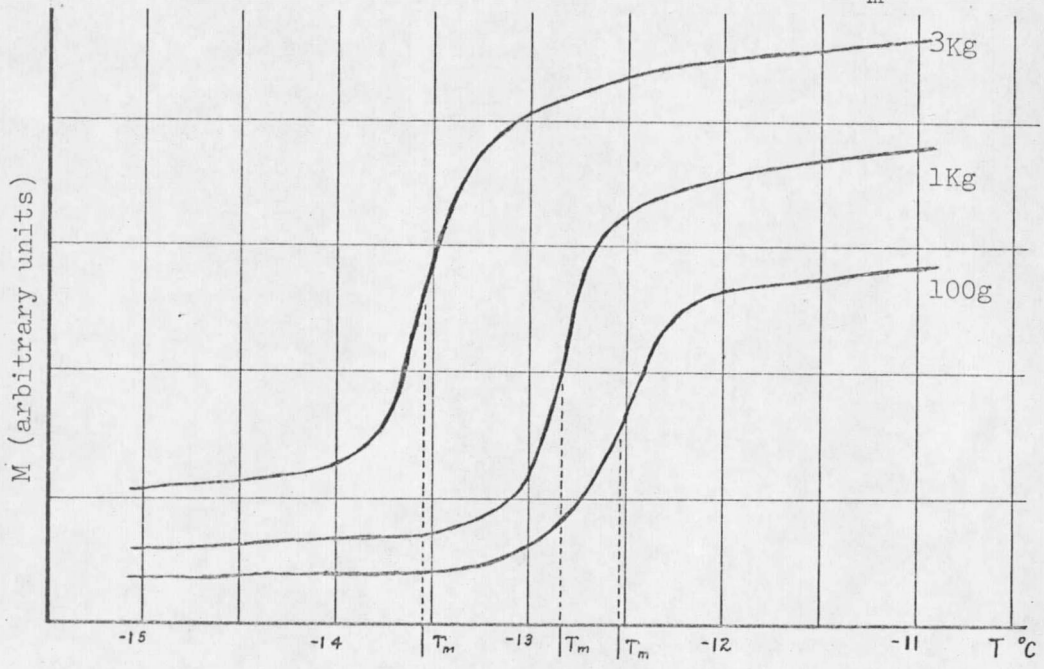


Fig. 4. Sample magnetization vs. temperature for several values of applied fields. All external fields are applied in the (111) plane.

The Morin transition may also be altered by adding metallic impurities by substitution in the lattice. In most cases the substitution of

impurities will either change $T_m$ or broaden the transition or both.[8] Analysis of the effects of impurities, however, is full of gross inconsistencies, even between dopings of similar spin composition. As a result of research at MSU, few, if any, conclusions may be drawn about impurity effects. This paper will report briefly on the calculated effect of impurities in the magnetic lattice as based on the model to be presented.

# CHAPTER II

# DESCRIPTION OF THE PROBLEM

By employing an extension of the phenomenological theory of J. O. Artman et. al.,[3,4] this paper will present a calculation that includes the effect of external fields on the crystalline anisotropy and hence the Morin transition of hematite. The basic assumption is, as already stated, that the transition occurs in coincidence with the anisotropy constant crossing zero. In order to perform the calculation, the effect of applied magnetic fields on the sublattice magnetizations and temperature dependence must be included, in addition to the anisotropy calculation.

The origin of the crystalline anisotropy in antiferromagnetic materials has three contributions: (1) the spin-orbit coupling between the spin and the orbital motion of the electrons, often called the fine-structure anisotropy, (2) the magnetic dipole-dipole interaction, and (3) an anisotropic exchange interaction between spins. The third term contributes a negligible amount to the total anisotropy energy in antiferromagnetic materials.[9] The other two terms are nearly equal in magnitude but, because of the magnetic geometry of hematite, they are opposite in algebraic sign.

Previous work in this area for the case of zero applied fields has been done by J. O. Artman[3] who developed a model using the fine-structure and dipolar energies. In his model the two terms are competing with each other to orient the spins either parallel or perpendicular to the c axis depending on whether their sum is positive or negative, respectively. The temperature dependence of each term has been calculated from quantum mechanical arguments by K. Yosida;[10] the derivation of these functions will be presented later.

The fine-structure anisotropy energy, which cannot be evaluated easily,

can be obtained from experimental data by subtracting the calculated dipolar anisotropy energy from the total anisotropy energy, which has been measured by antiferromagnetic resonance experiments. The anisotropy energy expression used by Artman was of the form:

$$K = K_{md}F_{md}(T) + K_{fs}F_{fs}(T), \qquad 2.1$$

where . . . $K$ = total anisotropy constant ($ergs/cm^3$)

$K_{md}$ = dipolar anisotropy constant for $T = 0°K$($ergs/cm^3$)

$F_{md}(T)$ = dipolar anisotropy temperature dependence

$K_{fs}$ = fine-structure anisotropy constant for $T = 0°K$($ergs/cm^3$)

$F_{fs}(T)$ = fine-structure anisotropy temperature dependence.

This model is, of course, only valid for temperatures below the Morin transition since it cannot account for the observed weak ferromagnetism in the temperature range between $T_m$ and the Néel temperature.

The model to be presented extends Artman's anisotropy model to include the effects of external magnetic fields. In order to do this, the assumption must be made that the internal molecular fields or crystalline fields are reasonably constant in magnitude through the transition. This assumption has been verified by recent Mössbauer studies of internal fields of hematite.[11] In addition, the model must assume that the crystalline fields are not sensitive to very small deviations in the canting angle ($\alpha$) from the antiferromagnetic condition. This situation occurs when the torque exerted on the magnetic moment by a field applied perpendicular to the c axis tends to rotate the dipole toward the field direction. This rotation is then opposed by a restoring torque from the crystalline field, which is

parallel to the c axis. The equilibrium condition is the zero of the torque expression:

$$\vec{W} = \vec{\mu} \times (\vec{H}_a + \vec{H}_{crys})$$

$$= \mu H_{crys} \sin \alpha - \mu H_a \cos \alpha = 0, \qquad 2.2$$

where $\mu$ is the magnetic moment, $H_{crys}$ is the crystalline field, and $H_a$ is the applied field. For a first-order approximation, the assumption seems to be valid since the perpendicular susceptibility is only slightly field dependent.[11]

With these two assumptions in effect, the additional term due to external fields is of the form:

$$K_{ex} = - \vec{\mu} \cdot \vec{H}_a , \qquad 2.3$$

where $K_{ex}$ is the energy due to external fields. The new expression for the total energy is then:

$$K = K_{md}F_{md}(T) + K_{fs}F_{fs}(T) + K_{ex}F_{ex}(T), \qquad 2.4$$

where $F_{ex}(T)$ expresses the temperature dependency of the external term. A detailed discussion of the temperature dependent functions will appear in the main portion of this paper.

Based on the model used in this paper, the effects of impurity cations on the dipolar anisotropy may be calculated by substituting ions of the impurity in the magnetic lattice. This calculation is only of casual interest since experimental evidence indicates that the impurity effects are not entirely magnetic in origin.[8]

# CHAPTER III

# CRYSTAL STRUCTURE AND LATTICE PARAMETERS

The dipolar contribution to the total anisotropy energy is highly dependent on the crystal structure, lattice parameters, and spin arrangement. Therefore, an accurate description of the hematite structure is necessary to perform the calculation. A direct summation method was chosen because of its simplicity and adaptability to electronic computers. This required the computation of the x, y, and z coordinates of enough magnetic ions to achieve good convergence of the dipolar anisotropy constant. A simple cartesian coordinate system was set up in which the orthogonal directions $[1\bar{2}1]$, $[10\bar{1}]$, and $[11\bar{1}]$ of the trigonal structure were chosen as the x, y, and z axes respectively.

Since the dipolar anisotropy energy is entirely magnetic in origin, the positions occupied by the oxygen anions is not important to the calculation. The contribution of these anions to the total anisotropy is included in the fine-structure term via the $\vec{S} \cdot \vec{L}$ coupling to the lattice. Therefore, only the magnetic lattice will be considered.

The diagram in Fig. 5 shows a projection along the $[10\bar{1}]$ axis onto the $(10\bar{1})$ plane taken from single crystal x-ray data for $\alpha$-$Fe_2O_3$ by Newnham and de Haan.[12] The closed circles are iron cations in the plane of the paper; the open circles are oxygen anions. The oxygen ions lie above or below the plane by the distances indicated in $\mathring{A}$.

A repetitive structural unit is formed by reflecting Fig. 5 through the plane of the paper, reversing all spin directions, and extending the result at the base of Fig. 5. The repetitive cell now contains twelve magnetic cations and eighteen oxygen anions. The twelve magnetic ions may be used to define a set of basis vectors for the repetitive magnetic

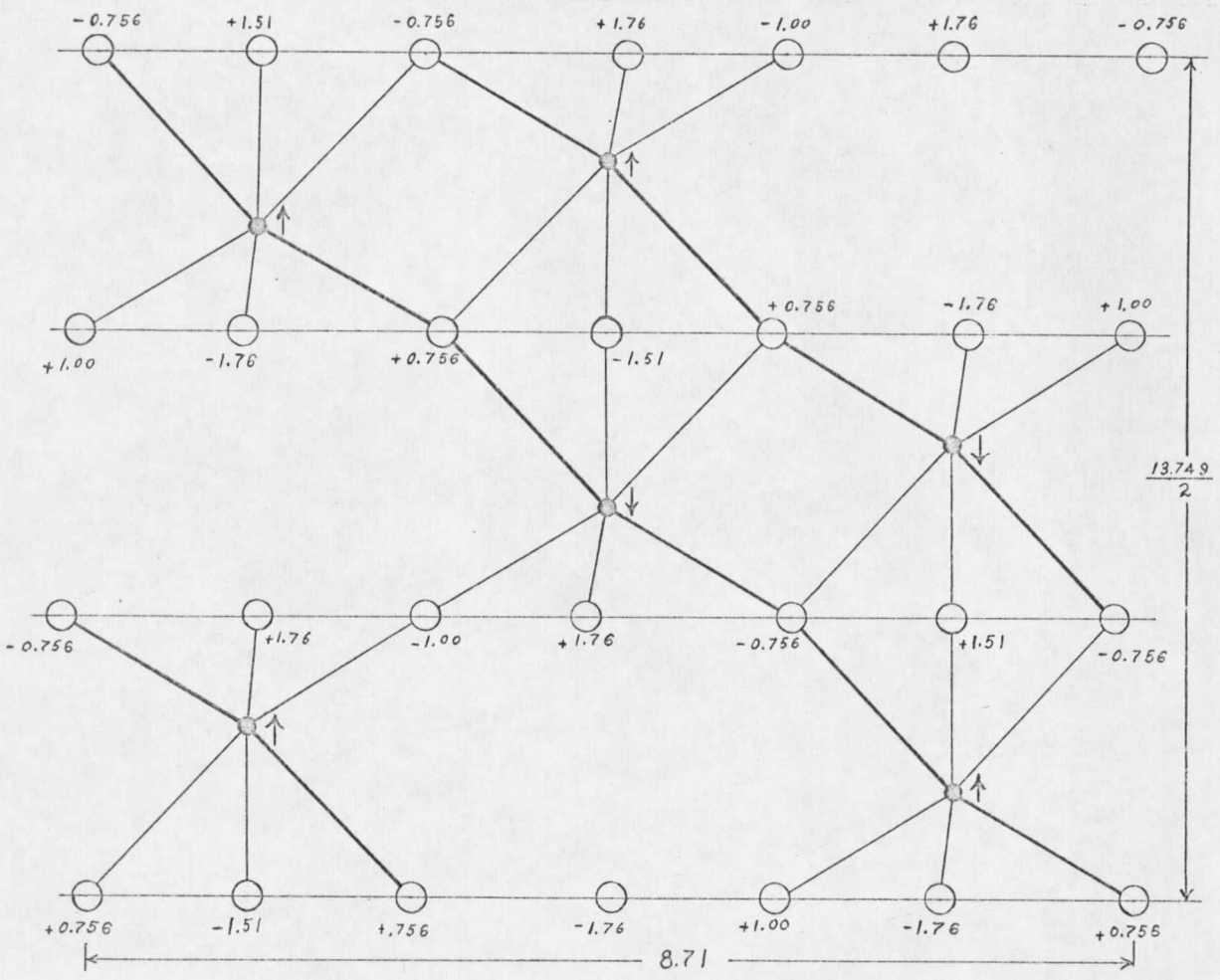


Fig. 5. Structure of $\alpha$-$Fe_2O_3$ as projected along the $[10\bar{1}]$ axis onto the $(10\bar{1})$ plane.

lattice. The basis is then added to Bravais lattice vectors that define the origins of the bases. The individual ion position vectors are given by

$$\vec{R}_{pk} = (\ell_p a_1 + B_{xk})\,\hat{i} + (m_p a_2)\,\hat{j} + (n_p a_3 + B_{zk})\,\hat{k} \qquad 3.1$$

where $a_1$, $a_2$, and $a_3$ are Bravais lattice constants, $B_{xk}$ and $B_{zk}$ are basis vector coordinates for the ion $k$ in the basis $p$, and $\ell_p$, $m_p$, and $n_p$

are positive or negative intergers. In addition, each ion in the basis was labeled + or - according to the sign of the associated spin.

Table 1. Basis vectors for $\alpha$-$Fe_2O_3$.

| k | $B_{xk}$(Å) | $B_{zk}$(Å) | Spin |
|---|---|---|---|
| 1 | 0.000 | 0.000 | + |
| 2 | 0.000 | -2.887 | - |
| 3 | -2.903 | -0.596 | + |
| 4 | 2.903 | 1.696 | - |
| 5 | 2.903 | -2.291 | - |
| 6 | -2.903 | 2.291 | - |
| 7 | 0.000 | 3.987 | + |
| 8 | -2.903 | -4.583 | + |
| 9 | 2.903 | 4.583 | + |
| 10 | 2.903 | -5.179 | + |
| 11 | 0.000 | -6.874 | - |
| 12 | -2.903 | 6.279 | - |

The calculated values of $B_{xk}$ and $B_{zk}$ appear in Table 1. The values for $a_1$, $a_2$, and $a_3$ were computed from crystallographic data[12] to insure proper positioning of the Bravais lattice sites; these values appear in Table 2.

Table 2. Bravais lattice parameters.

| $a_1$(Å) | $a_2$(Å) | $a_3$(Å) |
|---|---|---|
| 4.355 | 2.514 | 13.749 |

The actual quantities necessary for further calculations are the three

orthogonal position vector components, the magnitude of the position vector, and the sign of the spin at each ion site. This information was calculated for the 576 ions within a 15.1 Å radius of the central ion. The resulting cluster of ions was of nearly spherical symmetry; this would minimize extraneous shape effects. Machine program listings for the entire calculation are provided in the appendix.

# CHAPTER IV

# CALCULATION OF THE DIPOLAR FIELDS

The dipolar contribution to the effective magnetic field at any cation site, which is the origin of the dipolar anisotropy, is caused by the dipole moments of the neighboring ions. Since every ion site is magnetically similar, except for the sign of the spin, each dipole in the lattice has exactly the same anisotropy energy. The sign of the field vector at any ion site depends on the sign of the spin at that site; however, the field vector may be antiparallel to the dipole moment. This is the case for the antiferromagnetic phase in hematite. As a result, the dipolar anisotropy energy does not favor the antiferromagnetic condition; however, the dipolar field is parallel to the magnetic moment when the spins lie in the (111) plane.

An additional complication occurs when an external field cants the spin directions at an angle $\alpha$. This situation was discussed in Chapter II and will be treated in detail in the chapter on susceptibilities. The effect of this canting is to distort the magnetic symmetry causing a change in the direction and magnitude of the field at an ion site.

The dipolar field calculation then becomes a summation over the neighboring ions of the form:

$$\vec{H}_d = \sum_{i=1}^{N} p_i \left(-\frac{\vec{\mu}_\pm}{R_i^3} + \frac{(3\vec{\mu}_\pm \cdot \vec{R}_i)\vec{R}_i}{R_i^5}\right) , \qquad 4.1$$

where $p_i$ carries the sign of the magnetic moment i, $\vec{\mu}_\pm$ is the moment vector, and $\vec{R}_i$ is the position vector of the i'th ion site. The effect of spin canting is included by performing the calculations in a canted

coordinate system, then converting to the regular coordinates.

If a cartesian coordinate system is assumed, the magnetic moment and position vectors become:

$$\vec{\mu}_{\pm} = g\mu_{\beta} S(\sin\alpha\ \hat{i} \pm \cos\alpha\ \hat{k}) \qquad 4.2$$

and

$$\vec{R}_i = R_{xi}\ \hat{i} + R_{yi}\ \hat{j} + R_{zi}\ \hat{k}\ , \qquad 4.3$$

respectively, where g is the Landē factor, $\mu_{\beta}$ is the Bohr magneton, S is the spin quantum number, and the $R_{ki}$'s are the coordinates of $\vec{R}_i$. Eqn. 4.2 assumes that canting is allowed in the x-z plane only.

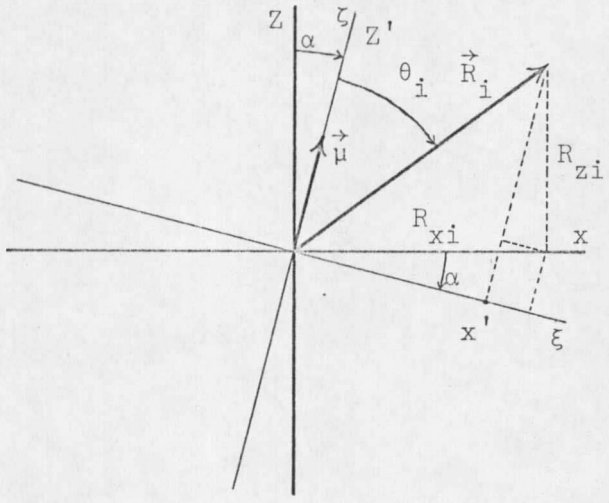


Fig. 6. Orientation of dipole moment in the canted (primed) coordinate system.

The angle, $\theta_i$, between $\vec{\mu}_{\pm}$ and $\vec{R}_i$ may be found from the dot product of the two vectors. It is less obvious that the azimuthal angle, $\Phi_i$, in the canted (primed) coordinate system, is a function of α. Considering the

diagram in Fig. 6,

$$x_i' = R_{xi} \cos \alpha - R_{zi} \sin \alpha \qquad 4.4$$

then:

$$\Phi_i = \cos^{-1}\left(\frac{x_i'}{|R_{xi}\,\hat{i} + R_{yi}\,\hat{j}|}\right), \qquad 4.5$$

where $\Phi_i$ lies in the plane normal to $\mu_\pm$. Eqn. 4.4 is valid for spin-up or spin-down by using $+\alpha$ or $-\alpha$, respectively.

The three components of the dipolar fields at the origin, in the canted coordinate system, become:

$$H_{xi}' = g\mu_\beta S_i \frac{3 \cos \theta_i \sin \theta_i \cos \Phi_i}{R_i^3} \qquad 4.6$$

$$H_{yi}' = g\mu_\beta S_i \frac{3 \cos \theta_i \sin \theta_i \sin \Phi_i}{R_i^3} \qquad 4.7$$

$$H_{zi}' = g\mu_\beta S_i \frac{3 \cos^2 \theta_i - 1}{R_i^3} \qquad 4.8$$

for the dipole moment $i$ with a position vector $\vec{R}_i$. The spin quantum number, $S_i$, is given a subscript to allow the substitution of impurity ions. Conversion to the direct coordinate system is done by operating on the canted coordinate system with a rotation matrix:

$$\begin{pmatrix} \cos\alpha & 0 & \sin\alpha \\ 0 & 1 & 0 \\ -\sin\alpha & 0 & \cos\alpha \end{pmatrix} \begin{pmatrix} H_{xi}' \\ H_{yi}' \\ H_{zi}' \end{pmatrix} = \begin{pmatrix} H_{xi} \\ H_{yi} \\ H_{zi} \end{pmatrix}, \qquad 4.9$$

for the spin up case; the spin down case requires the substitution of $-\alpha$

in Eqn. 4.9.

The total magnetic field vector components are formed by summing over all ions in the cluster. Hence

$$\vec{H} = \sum_{i=1}^{N} p_i (H_{xi}\,\hat{i} + H_{yi}\,\hat{j} + H_{zi}\,\hat{k}) \qquad 4.10$$

where $p_i$ carries the sign of the dipole moment i. The above summation was performed for 575 ions in a spherical cluster about the origin, not including the ion at the origin.

The summation converges very rapidly since it is of the form $\sum \pm \frac{1}{r^3}$. For the number of ions used, the sum is at least as accurate as the crystal data. For example, the last terms in the series are about two orders-of-magnitude smaller than the first terms. Thus, two or three figures in the total sum are significant.

# CHAPTER V

# THE TEMPERATURE DEPENDENT FUNCTIONS

In the usual molecular field theory of antiferromagnetism, the effective field at a cation site is given by:

$$\vec{H}_{eff} = -\gamma_1 \vec{M}_1 - \gamma_2 \vec{M}_2 + \vec{H}_a, \qquad 5.1$$

where the $\gamma_i$'s are the molecular field constants for each sublattice, the $\vec{M}_i$'s are the sublattice magnetizations, and $H_a$ is the applied field. Since antiferromagnetism requires that $|\vec{M}_1| = |\vec{M}_2| = M_o$, Eqn. 5.1 may be written as:

$$\vec{H}_{eff} = -\gamma_o \vec{M}_o + \vec{H}_a, \qquad 5.2$$

where $\gamma_o = \gamma_1 + \gamma_2$. The constant $\gamma_o$ may be evaluated by expressing the Heisenberg exchange Hamiltonian in terms of the molecular field[13]; hence;

$$\underline{H} = -g\mu_\beta S_{zi} \gamma_o M_o = -2J_e \sum_{ij} S_{zi} S_{zj}, \qquad 5.3$$

where $S_{zi}$ and $S_{zj}$ are the spin quantum numbers of the atom i and the nearest neighbor j, respectively, and $J_e$ is the exchange integral. Performing the summation over z nearest neighbors and setting $M = \frac{Ng\mu_\beta S_{zj}}{2}$ gives:

$$\gamma_o = \frac{4zJ_e}{Ng^2\mu_\beta^2}, \qquad 5.4$$

where N is the ferric ion concentration.

In an antiferromagnetic material, the exchange integral is always negative; therefore, the effective field may be written in the form:

$$\vec{H}_{eff} = \frac{4z|J_e|}{Ng^2\mu_\beta^2} \vec{M}_o + \vec{H}_a, \qquad 5.5$$

where the product $z|J_e|$ has to be evaluated.

At the condition of thermal equilibrium, the sublattice magnetization is the statistical average, over all spin states, of the dipole moment per unit volume. Assuming the dipoles can be treated independently, the magnetization is then given by:

$$\bar{M} = \frac{N}{2} \frac{\sum_{-S}^{+S} M_S g\mu_\beta \exp(-\frac{M_S g\mu_\beta H_{eff}}{kT})}{\sum_{-S}^{+S} \exp(-\frac{M_S g\mu_\beta H_{eff}}{kT})}, \qquad 5.6$$

where N is the number of iron ions per $cm^3$, k is Boltzmann's constant, $H_{eff}$ is the field acting on the dipole moment, and $M_S = -S, -S+1, \ldots, +S$. Performing the summation yields:

$$M(T) = \frac{Ng\mu_\beta S}{2} [\frac{2S+1}{2S} \coth (\frac{2S+1}{2S}X) - \frac{1}{2S} \coth \frac{X}{2S}], \qquad 5.7$$

where

$$X = \frac{g\mu_\beta S H_{eff}}{kT}. \qquad 5.8$$

The quantity in brackets is the well-known Brillouin function which defines the temperature dependency of the spontaneous magnetization. This function is usually written as $B_s(x)$. Since the argument is a function of $M_o(T)$, the function is solvable only by some type of iterative method.

As the temperature of the sample approaches the Néel temperature, $B_s(x)$ goes to zero as the crystal loses its magnetization. For small values of $x(x<<1)$ the Brillouin function may be expanded about $x = 0$ which yields:

$$M_o(T) = \frac{Ng\mu_\beta S}{2}\left[\frac{S+1}{3S}X - \frac{S+1}{3S}\frac{2S^2+2S+1}{30S^2}X^3 + \ldots\right]. \qquad 5.9$$

Substituting $H_{eff} = \gamma_o M_o(T)$ into Eqn. 5.8 and eliminating $M_o(T)$ with the first term of Eqn. 5.9 yields for the Néel temperature:

$$T_N = -\frac{Ng^2\mu_\beta^2 \; S(S+1)}{6k}\gamma_o . \qquad 5.10$$

By using Eqn. 5.4 and Eqn. 5.10 the product $z|J_e|$ becomes:

$$z|J_e| = \frac{3kT_N}{2S(S+1)} . \qquad 5.11$$

The substitution of Eqn. 5.11 into Eqn. 5.5 yields the effective field:

$$\vec{H}_{eff} = \frac{3kT_N}{S(S+1)g\mu_\beta}\vec{S} + \vec{H}_a , \qquad 5.12$$

which is expressed entirely in externally measurable quantities.

The temperature dependence of the magnetic moment is then given by $\mu_\pm(T) = g\mu_\beta S\, B_s(x)$. This means that $F_{ex}(T)$, from Eqn. 2.3, is simply $B_s(x)$, since the external field is independent of temperature. On the other hand, the dipolar anisotropy is proportional to $[\mu_\pm(T)]^2$, since it is of the form $K \propto \vec{\mu}_\pm \cdot \vec{H}_{md}$, and $F_{md}(T)$, from Eqn. 2.3, is equal to $B_s^2(x)$.

The fine-structure anisotropy energy originates from the coupling between the spin and the orbital motion of the electrons. In the spin Hamiltonian for uniaxial symmetry, this energy appears as a term of the form:[14]

$$\underline{H} = -DS_z^2 , \qquad 5.13$$

where $\underline{H}$ is the single ion Hamiltonian, D is the fine-structure coupling constant, and $S_z$ is the component of spin in the easy direction. If the

axis of quantization deviates from the easy direction by an angle $\alpha$, then the overall fine-structure anisotropy energy for the crystal is given by:

$$K_{fs} F_{fs}(T) = \sum_i - D_i \overline{S_{zi}^2} = - D \sum_i \overline{S_{zi}^2} , \qquad 5.14$$

where the summation is carried over all ions in the crystal, and $\overline{S_z^2}$ is the average value of $S_z^2$ in the canted eigenstate.

The temperature dependence of $K_{fs}$ may be derived by the following considerations.[10] Assume, as in Fig. 6, that the axis of spin quantization ($\zeta$-axis) is allowed to deviate from the easy axis (z-axis) by an angle $\alpha$. In addition, define the axes $\eta$, $\xi$, and $\zeta$ as an orthogonal right-handed coordinate set in the canted system. Then the quantity $S_z^2$ may be written:

$$\begin{aligned} S_z^2 &= (S_\zeta \cos\alpha + S_\xi \sin\alpha)^2 \\ &= [S_\zeta^2 \cos^2\alpha + S_\xi^2 \sin^2\alpha + \sin\alpha \cos\alpha (S_\zeta S_\xi + S_\xi S_\zeta)]. \end{aligned} \qquad 5.15$$

The third term in Eqn. 5.15 is identically zero by anticommutation; the other terms are considered separately below. If $\psi_M$ is the eigenstate in which $S_\zeta$ has its eigenvalue M, then for the first term of Eqn. 5.15 the average value of $S_\zeta^2$ is given by:

$$\langle \psi_M | S_\zeta^2 | \psi_M \rangle = \overline{M^2} \quad . \qquad 5.16$$

Also, from the relation for the components of spin angular momentum:

$$\overline{S^2} = \overline{S_\eta^2} + \overline{S_\xi^2} + \overline{S_\zeta^2} \quad ,$$

the following equation is obtained by substituting for $\overline{S^2}$:

$$S(S+1) = 2\,\overline{S_\xi^2} + \overline{S_\zeta^2} \quad ,$$

where it is assumed that $\overline{S_\eta^2} = \overline{S_\xi^2}$. This gives for the second term of Eqn. 5.15:

$$\langle\psi_M|S_\xi^2|\psi_M\rangle = \frac{1}{2}[S(S+1) - \overline{M^2}] \quad . \qquad 5.17$$

Using Eqns. 5.16 and 5.17 with the identity yields for the statistical average of $S_z^2$ in the state $\psi_M$:

$$\langle\psi_M|S_z^2|\psi_M\rangle = [(\cos^2\theta - \frac{1}{2}\sin^2\theta)\overline{M^2} + \frac{1}{2}S(S+1)\sin^2\theta]. \qquad 5.18$$

The value of $\overline{M^2}$ may be calculated by a method entirely similar to the previous calculation of $\bar{M}$ in Eqn. 5.6. Performing the summation is quite lengthy; therefore, the result will be quoted as:[10]

$$\overline{M^2} = [S(S+1) - S\,B_s(x)\coth\frac{x}{2S}]. \qquad 5.19$$

Substitution of Eqn. 19 into Eqn. 18 gives, after normalization at T = 0°K, the final temperature dependency of the fine-structure anisotropy energy which is:

$$F_{fs}(T) = \frac{1}{2S-1}[2(S+1) - 3\,B_s(x)\coth\frac{1}{2S}x]. \qquad 5.20$$

The three temperature functions previously derived are all equal to unity at T = 0°K and zero at the Néel temperature. This is as expected since all antiferromagnetic properties of a crystal are lost at $T_N$ and all functional dependence on temperature must disappear at T = 0°K. $F_{ex}(T)$ and $F_{md}(T)$ are valid for all values of S and T between $0 < T \leq T_N$. $F_{fs}(T)$

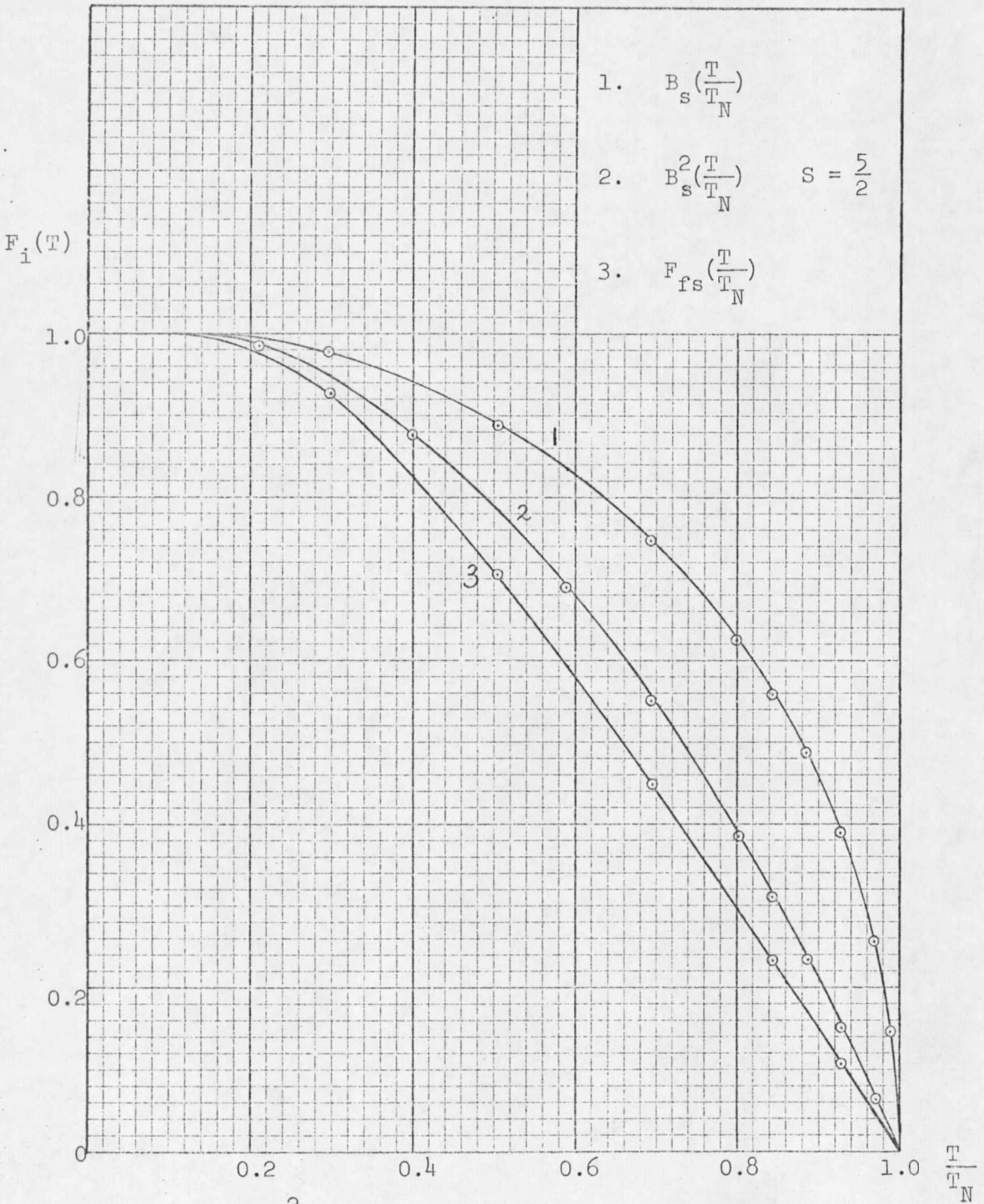


Fig. 7. $B_s(x)$, $B_s^2(x)$ and $F_{fs}(x)$ as a function of $T/T_N$.

is valid over the same temperature range; however it is invalid for $S = \frac{1}{2}$ and must be considered identically zero, since for $S = \frac{1}{2}$ there is no orbital momentum. Hence, the spin-orbit interaction does not exist. The three curves in Fig. 7 show the relationship between the normalized temperature dependent functions.

# CHAPTER VI

# MAGNETIC SUSCEPTIBILITY

In the preceding chapter, the effect of temperature on the magnetic moment was given by the Brillouin function $B_s(x)$, where x is a function of both the temperature and the effective field ($H_{eff}$) acting on the dipole. In the present case, $H_{eff}$ is the vector sum of three different fields: (1) the exchange field of Eqn. 5.12, (2) the dipolar field of Eqn. 4.10, and (3) the external field applied perpendicular to the antiferromagnetic axis. Of these three contributions, only (1) and (2) are temperature dependent; this results in a component of $H_{eff}$ that is independent of $B_s(x)$. The effect of the temperature independent term has been investigated by including it in the effective field of the Brillouin function. Thus, $H_{eff}$ becomes:

$$|H_{eff}| = |(H_{exc} + H_z) B_s(x) \hat{k} + (H_x B_s(x) + H_a) \hat{i}| , \qquad 6.1$$

where $H_{exc}$ is the exchange field, and $H_x$ and $H_z$ are the dipolar fields from Chapter IV. For the applied fields commonly used in the laboratory, <15 koe, the effect, however, is entirely negligible since the exchange field is so large, about $10^6 - 10^7$ oe. The same reasoning applies to the negligibility of $H_z$ and $H_x$ in Eqn. 6.1 since their orders of magnitude are $<10^4$ oe. and $10^2$ oe., respectively.

The tendency of the applied fields to cant the magnetic moments away from antiferromagnetism has been discussed previously. The magnitude of $\alpha$, the canting angle, may now be calculated by considering the torque on a dipole in a magnetic field. Solving for the zero of Eqn. 2.2 gives the obvious solution for $\alpha$:

$$\alpha = \mathrm{Tan}^{-1}\left(\frac{H_x B_s(x) + H_a}{H_{exc} B_s(x) + H_z B_s(x)}\right). \qquad 6.2$$

Based on the simple torque model given above, the perpendicular mass susceptibility, for an antiferromagnetic material is given by:

$$\chi_\perp = \frac{N g \mu_\beta S \sin\alpha}{\rho} \; \frac{\text{ergs}}{\text{gm-Oe}^2}, \qquad 6.3$$

where $\rho$ is the density of the sample.

J. H. Van Vleck[15] has given another interpretation of the susceptibility based on the change of the spin vector induced by the components of the external field parallel and perpendicular to the original spin direction. His theory is perhaps more pleasing from a mathematical point of view since he has included the increase of the dipole moment when a field is applied. However, for the case of external fields that are small compared to the exchange field, the additional correction is negligible.

The present model gives a value for the mass susceptibility of $\chi_\perp = 58.8\times10^{-5} \frac{\text{erg}}{\text{gm-oe}^2}$ which is about 3 times as large as the experimental value of Néel and Panthenet.[7] This result is not too surprising since the exchange fields were assumed independent of $\alpha$.

# CHAPTER VII

# THE TOTAL ANISOTROPY ENERGY

As stated in the introduction, the Morin transition can be phenomenologically described by a change of sign of the anisotropy constant. This approach can lead to a transition only if the magnetic dipole and the fine-structure contributions to the total anisotropy are of opposite sign. Using the first-order definition of the total uniaxial anisotropy energy, as expressed by Eqn. 1.1, implies that K is positive below the transition since the spins are collinear with the c axis. The magnitude of K for hematite has been measured, for low temperatures, and found to be approximately $2.0 \times 10^5 \frac{\text{erg}}{\text{cm}^3}$.[3] In the remainder of this section, each contribution to the total anisotropy energy will be considered separately.

The magnetic dipolar anisotropy per ion is given by:[3]

$$F = -\frac{1}{2}\vec{\mu} \cdot \vec{H}_d = -\frac{1}{2}\mu H_d\left(\frac{3\cos^2\theta - 1}{2}\right) \qquad 7.1$$

where F is a free energy, $\theta$ is the angle between $\vec{\mu}$ and the c axis, and $H_d$ is the dipolar field. When expressed in terms of the notation of Eqn. 1.1, the angular dependent term of Eqn. 7.1 becomes:

$$F = \frac{3}{4} g\mu_\beta S H_d \sin^2\theta \qquad 7.2$$

$$= K_{md} \sin^2\theta \quad ,$$

where $K_{md} = \frac{3}{4} g\mu_\beta S H_d$ is the single ion dipolar anisotropy constant. For the magnetic geometry of hematite, the dipolar field is antiparallel to the magnetic moment when the spins are parallel to the c axis. If $\vec{\mu}$ is assumed in the positive direction, then $H_d$ and $K_{md}$ are both negative. The result of Eqn. 7.2 is valid only at $T = 0^\circ K$; the temperature dependence of

$K_{md}$ has been discussed previously in Chapter 5.

The fine-structure contribution to the anisotropy energy is not as easy to calculate as the dipolar term. However, since the total anisotropy is the sum of $K_{md}$ and $K_{fs}$, the fine-structure term may be evaluated by subtracting the dipolar anisotropy energy from the experimentally measured total anisotropy energy, thus:

$$K_{fs} = K - K_{md}\Big|_{T=0^\circ K}. \qquad 7.3$$

Again, the temperature dependence of $K_{fs}$ has been discussed previously in Chapter 5.

The additional energy term that includes the effect of the external field on the free energy is given by the usual expression for the energy of a dipole in a magnetic field:

$$K_{ex} = -\vec{\mu}_{\pm} \cdot \vec{H}_a = -g\mu_\beta S H_a \cos(90^\circ-\alpha)$$

$$= -g\mu_\beta S H_a \sin\alpha. \qquad 7.4$$

This term has an effect that is similar to an extrinsic anisotropy. Since it depends only on the strength of the external field, which is temperature independent, and the magnetic moment, its temperature dependence is simply that of the dipole moment.

The actual value of the applied field at the dipole site is not the same as the external, applied magnetic field. Due to the uncompensated poles of the induced magnetization in the direction of the external field, a demagnetizing field arises which tends to reduce the external field. Assuming spherical samples, if $H_{ext}$ is the field external to the crystal,

then:

$$\vec{H}_a = \vec{H}_{ext} - D\vec{M}_i \quad , \qquad 7.5$$

where D is the scalar demagnetizing factor for a spherical sample and $M_i$ is the induced magnetization from $H_{ext}$.

The total anisotropy is now given by multiplying each contribution by its respective temperature dependent function and adding the three products. It should be noted that the phrase "total anisotropy" refers only to the first-order model used in this paper. This is not meant to imply that the sum of $K_{md}$, $K_{fs}$, and $K_{ex}$ completely describes the anisotropy of an antiferromagnetic crystal. In equation form:

$$K = K_{fs}F_{fs}(T) + K_{md}B_s^2(x) + K_{ex}B_s(x) \quad , \qquad 7.6$$

where $F_{fs}(T)$ is the fine-structure temperature function of Eqn. 5.20.

The value of $T_m$, for a given applied field, may be calculated by hunting for the first zero of Eqn. 7.6 with respect to temperature. A plot of K as a function of temperature for zero applied field appears in Fig. 8. For non-zero applied fields, the curve in Fig. 8 is shifted downward slightly; the amount of the shift may be seen from Fig. 9 which has a greatly expanded temperature scale and includes only a small portion of Fig. 8.

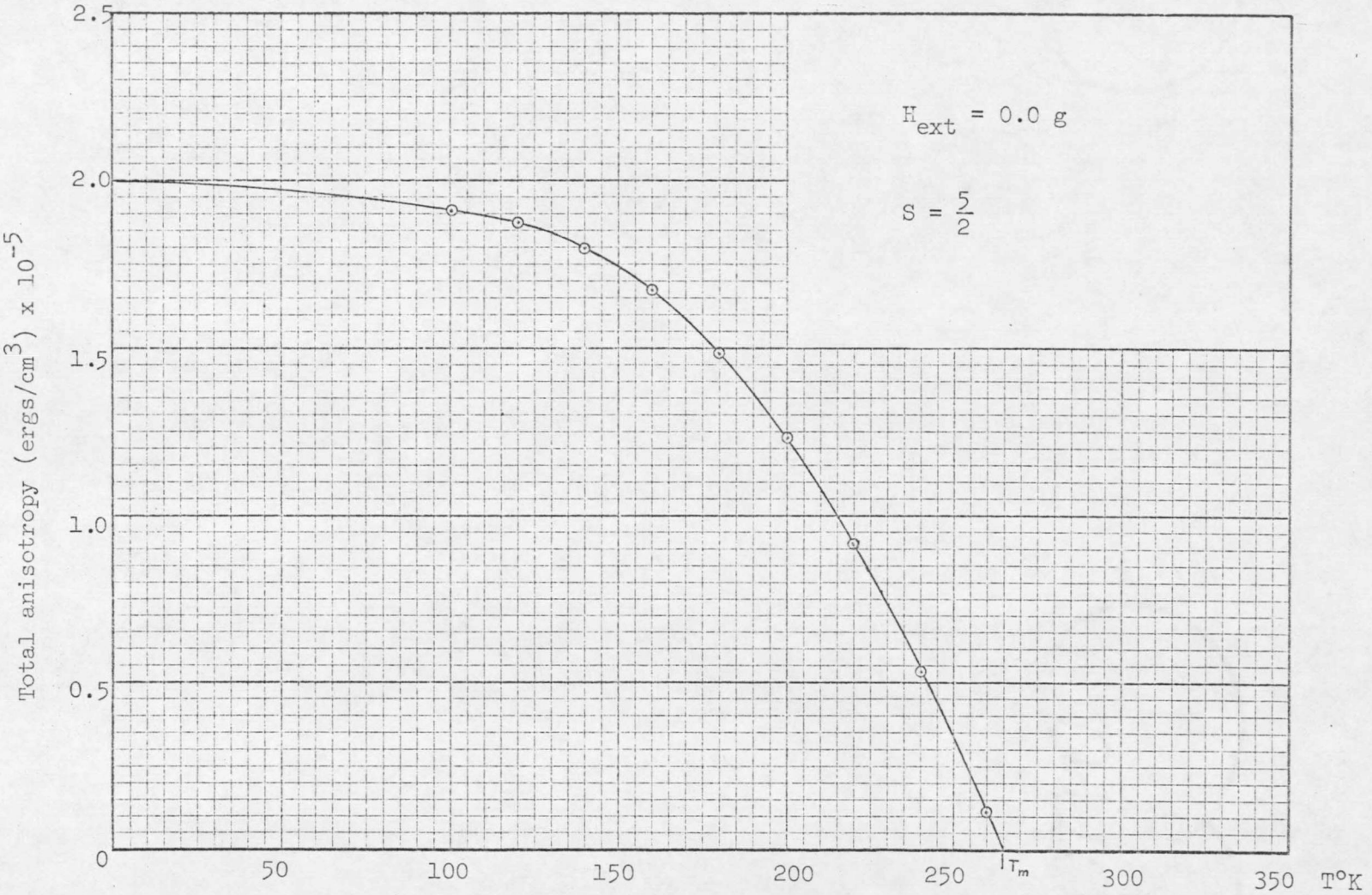


Fig. 8. Total anisotropy for all temperatures below $T_M$.

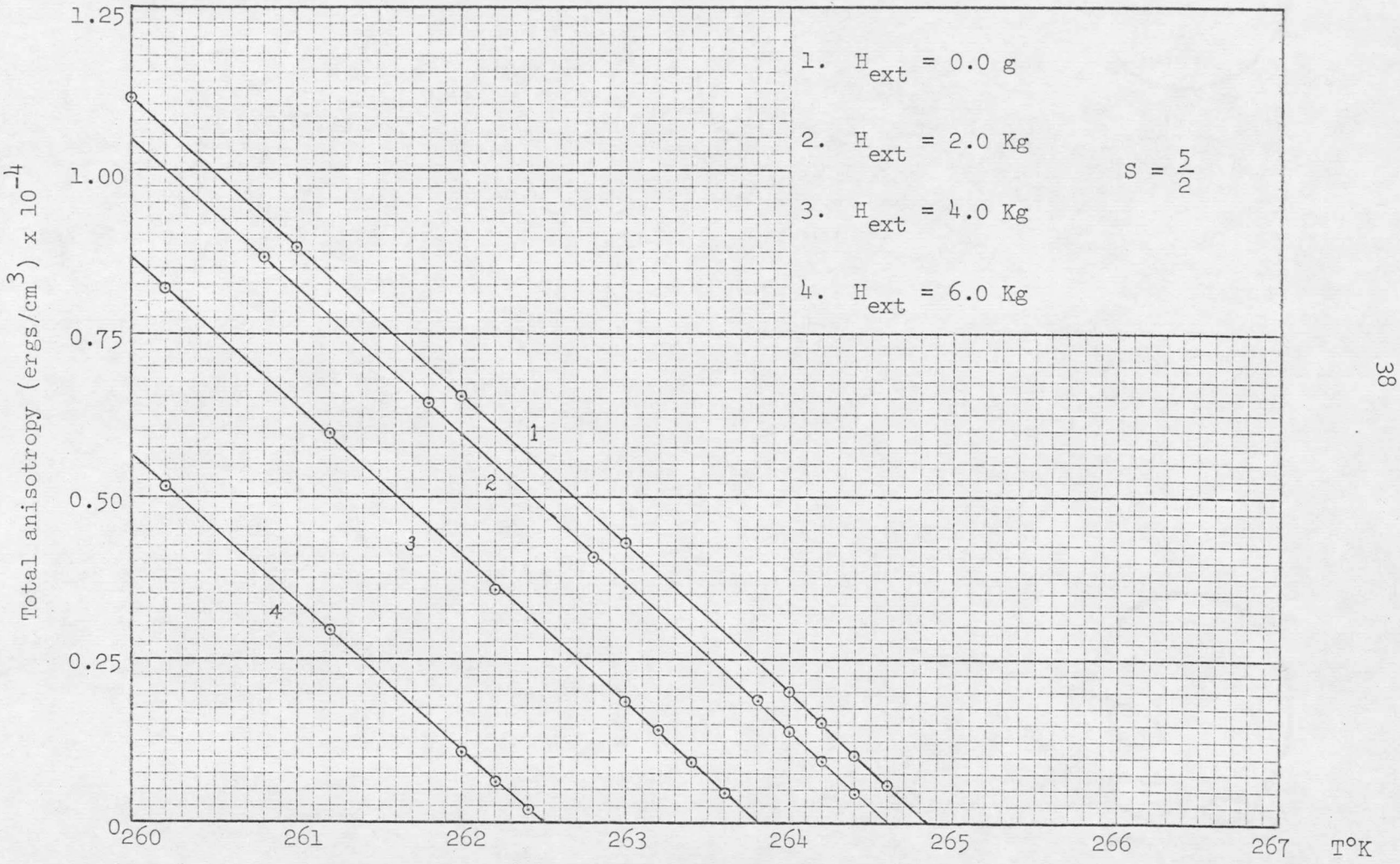


Fig. 9. Total anisotropy near the transition temperature.

# CHAPTER VIII

# COMPARISON TO EXPERIMENTAL RESULTS

The zero of Eqn. 7.6, for a given external field, indicates the value of $T_m$ predicted by this model. The nominal value of $T_m$ for zero applied fields from Fig. 9 is about -8°C which compares favorably with the experimental value of -12°C extrapolated from Fig. 4. Fig. 9 also shows a shift that is of the same order of magnitude as the experimental results; however, one can note that the calculated shift is nearly proportional to the square of the applied field. Nearly all experimental results indicate a linear relationship between $\Delta T$ and $H_{ext}$.[8] The nonlinearity of Fig. 9 and Eqn. 7.6 is caused by the additional term which contains $H_a$ and sin $\alpha$, both of which are almost linearly proportional to $H_{ext}$. This results in $K_{ext}$ being proportional to $H_{ext}^2$.

The graph in Fig. 10 shows the sample magnetization as a function of temperature for several values of applied fields; the vertical line indicates the discontinuous jump in magnetization at the Morin transition. In this diagram the "square-law" dependence of $\Delta T$ is very apparent. Since the problem is concerned with the dipolar fields and fine-structure interactions of one single dipole, the transition appears to be instantaneous. Actually, lattice inhomogenities would tend to broaden the apparent transition when the total magnetization of a crystal is measured. This would account for the finite slope of the discontinuity in Fig. 4.

The effect of impurity ions on the local magnetic fields was investigated by substituting ions with different spin quantum numbers in the dipolar summation. This resulted in an increase or decrease in $T_m$ depending on the location of the impurity ion. For example, any of the

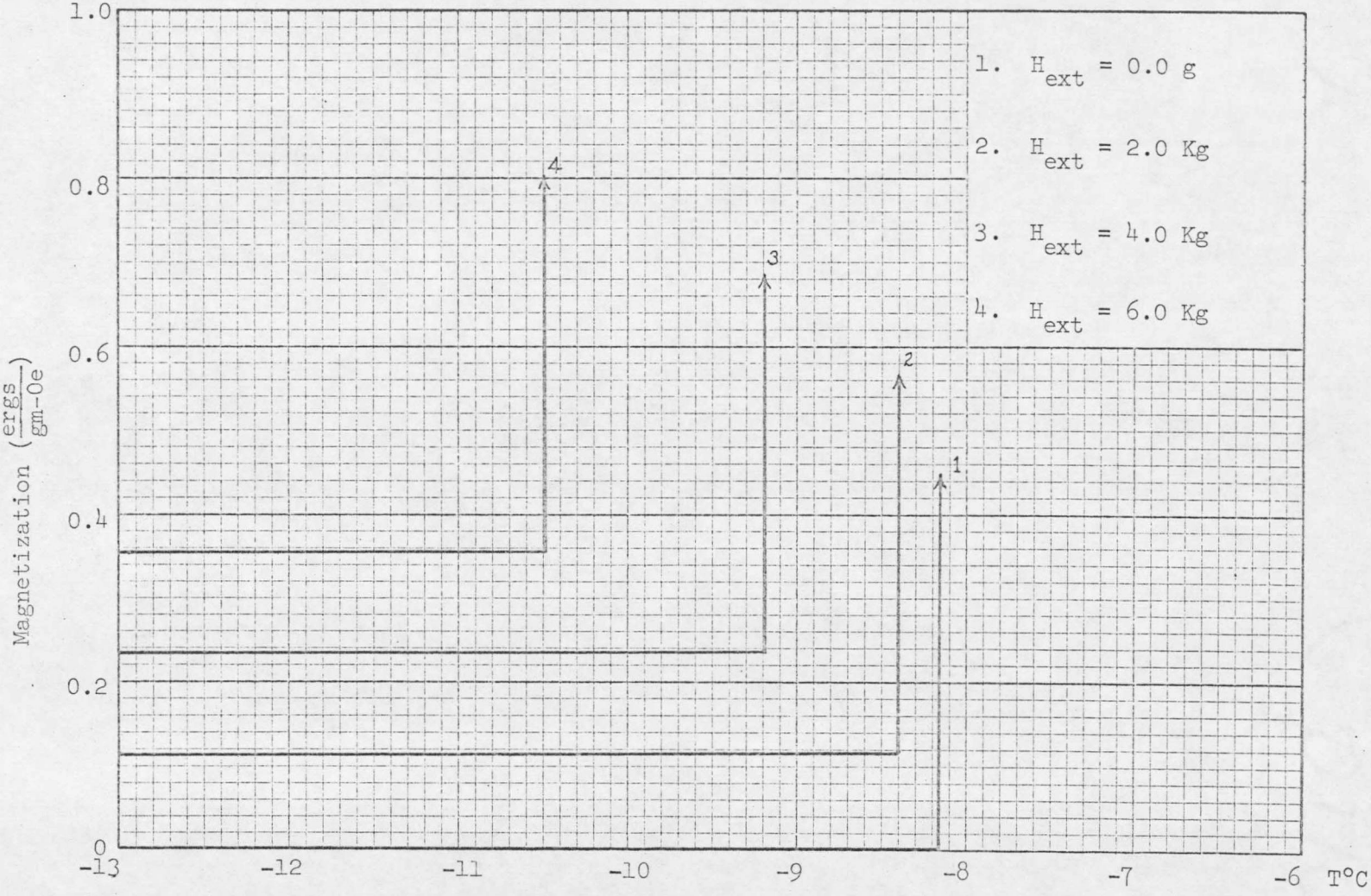


Fig. 10. Magnetization of bulk sample for given external field.

first four nearest neighbors would increase the nominal value of $T_m$ when a $Cr^{3+}$ ion (S = 3/2) was substituted in place of $Fe^{3+}$ (S = 5/2). On the average, all other ions in the lattice would tend to decrease the value of $T_m$, but to a lesser degree. As a result, this dipolar model would predict an increase of $T_m$ for impurities with $S < 5/2$ and a decrease of $T_m$ for impurities with $S > 5/2$. The actual experimental results indicate that all dopings tend to decrease the value of $T_m$.[8] This would indicate that the effect of impurities on the transition temperature is not primarily a dipolar field effect. The depression of $T_m$ by impurities is more likely caused by distortion of the crystal lattice and the electronic wave functions by the foreign ion.

# CHAPTER IX

# CONCLUSIONS

The calculated results of Eqn. 7.6, that appear in Figs. 9 and 10, indicate a depression of the Morin transition temperature with increasing applied fields. The predicted nominal value of $T_m$ and the approximate magnitude of the calculated depression both compare very favorably with experimental data.[8] While the experimental evidence shows a linear relationship, the calculation predicts that $\Delta T$ would be nearly proportional to the square of the external field. This would indicate that the additional energy term is not the only factor contributing to the effect.

In order to improve the model used in this calculation, the first and most obvious step would be to calculate the effect of the canting angle $\alpha$ on the fine-structure anisotropy energy and the exchange interaction, both of which were assumed independent of $\alpha$. Since both terms have their origin in the overlap of wave functions, it is reasonable to assume that the amount of overlap would be highly dependent on the canting angle. A calculation of this type may tend to linearize the results of Eqn. 7.6, since it would apply to the anistropy term which is independent of all applied fields. Unfortunately, such a calculation would be extremely difficult to perform in detail.

As mentioned before, the effect of impurities on the value of $T_m$ cannot be predicted by this dipolar field model. The substitution of $Cr^{3+}$ impurities ($S=\frac{3}{2}$) in the lattice had an overall effect of raising the transition temperature. Actually, experimental results indicate a decrease of the transition temperature when any impurity is substituted into the magnetic lattice.[8] However, the experimental evidence

available is for doping concentration of the order of 1% substitution. Perhaps higher dopings would indeed elevate the transition temperature.

# APPENDIX

## MACHINE PROGRAM LISTINGS

```
MACHINE PROGRAM FOR CALCULATION OF LATTICE PARAMETERS
DATA OUTPUT CARDS  RX,RY,RZ,R,R3,N
   DIMENSION R(1501),RZ(1501),RX(1501),RY(1501),SGN(1501)
   DIMENSION  X(12),Z(12),AJ(12)
 1 L=1
READ BASIS VECTORS
 2 READ 19,X(L),Z(L),AJ(L)
   IF(X(L)-1.0) 3,24,3
 3 IF(L-12) 4,5,5
 4 L=L+1
   GO TO 2
 5 I=0
READ BRAVAIS LATTICE CONSTANTS
   READ 20,DX,DY,DZ
READ  NUMBER OF ION LOCATIONS DESIRED
   READ 23, NCDS
READ  BRAVAIS LATTICE MULTIPLIERS
 6 READ 21,AX,AY,AZ
   IF(AX-99.0) 7,9,9
 7 RXI=DY*AX
   RYI=DY*AY
   RZI=DZ*AZ
   DO 8 K=1,12
   J=I+K
   RX(J)=RXI+X(K)
   RZ(J)=RZI+Z(K)
   RY(J)=RYI
 8 SGN(J)=AJ(K)
   I=I+12
   GO TO 6
 9 DO 10 I=1,J
   R2=RX(I)**2+RY(I)**2+RZ(I)**2
10 R(I)=SQRTF(R2)
SORT IN NUMERIC ORDER WRT RADIUS
   I=1
   K=1
11 IF(R(K)-R(I)) 12,13,13
12 A=RX(I)
   RX(I)=RX(K)
   RX(K)=A
   A=RY(I)
   RY(I)=RY(K)
   RY(K)=A
   A=RZ(I)
   RZ(I)=RZ(K)
   RZ(K)=A
   A=R(I)
```

```
      R(I)=R(K)
      R(K)=A
      A=SGN(I)
      SGN(I)=SGN(K)
      SGN(K)=A
   13 IF(K-J) 14,15,15
   14 K=K+1
      GO TO 11
   15 I=I+1
      K=I
      IF(I+K-2*J) 11,16,16
  OUTPUT
   16 DO 17 I=1,NCDS
      R3=R(I)**3
   17 PUNCH 22,RX(I),RY(I),RZ(I),R(I),R3,SGN(I),I
   18 GO TO 1
   19 FORMAT (2E16.8,F5.1)
   20 FORMAT (3E14.7)
   21 FORMAT (3F5.1)
   22 FORMAT (5E14.7,F5.1,I5)
   23 FORMAT(I5)
   24 CALL EXIT
      END
```

```
MACHINE PROGRAM FOR CALCULATION OF MORIN TEMPERATURE
    DOUBLE PRECISION  X1,X2,HA,HB,HC,HD,BX,DBX,X
    DOUBLE PRECISION A1,B1,C1,HEXC,HIND,BX1
    DIMENSION RX(600),RY(600),RZ(600),R(600),R3(600),SGN(600)
    DIMENSION UBX(21),NI(21),N(600)
 1  I=1
READ - ION LOCATION AND SPIN SIGN FOR N IONS
 2  READ 23,RX(I),RY(I),RZ(I),R(I),R3(I),SGN(I),N(I)
    IF(RX(I)-1.0) 4,8,4
 4  I=I+1
    GO TO 2
 8  J=I-1
READ - BOHR MAGNETON, UB PER DIPOLE, 1.0E-24
    READ 24,UB,UBN,RRR
    I=1
READ - UB PER IMPURITY ION, IMPURITY ION NUMBER
 9  READ 25,UBX(I),NI(I)
    IF(UBX(I)-99.0) 10,11,11
10  I=I+1
    GO TO 9
11  NIMP=I-1
READ - SUBLATTICE (-1.0,0.0,OR 1.0)
    READ 25,SUB
READ - SPIN QN, BOLTZMANN CONSTANT
    READ 23,S,BK
READ - NEEL TEMP, TEMP INCREMENT, INITIAL TEMP, FINAL TEMP
43  READ 23,TN,DT,TI,TH
READ - EXTERNAL FIELD PERPENDICULAR TO SPIN
    READ 23,HAPL1
    IF(HAPL1) 47,45,45
45  ALPHA=0.0
    CVEX=1.0
CALCULATE DIPOLAR FIELDS
12  HX=0.0
    HY=0.0
    HZ=0.0
    I=2
13  IF(SGN(I)-SUB) 5,6,5
 5  ALPHA=ABSF(ALPHA)*SGN(I)
    UX=SINF(ALPHA)
    UZ=COSF(ALPHA)
    AA=(ABSF(UX)*(RX(I)-RX(1))+UZ*SGN(I)*(RZ(I)-RZ(1)))/R(I)
    IF(AA**2-1.0)3,3,7
 7  AA=1.0
 3  BB=SQRT(1.0-AA**2)
    X3=(RX(I)-RX(1))*UZ-(RZ(I)-RZ(1))*UX
    R1=SQRTF(X3**2+(RY(I)-RY(1))**2)
```

```
      IF(R1) 15,14,15
   14 CC=0.0
      DD=0.0
      GO TO 16
   15 CC=X3/R1
      DD=(RY(I)-RY(1))/R1
   16 HE=3.0*AA*BB*CC/R3(I)
      HG=3.0*AA*BB*DD/R3(I)
      HH=(3.0*AA**2-1.0)/R3(I)
      DO 18 K=1,NIMP
      IF(N(I)-NI(K)) 18,17,18
   17 HE=HE*UBX(K)/RRR
      HG=HG*UBX(K)/RRR
      HH=HH*UBX(K)/RRR
      GO TO 19
   18 CONTINUE
      HE=HE*UBN/RRR
      HG=HG*UBN/RRR
      HH=HH*UBN/RRR
   19 HX=HX+SGN(I)*(HE*UZ+HH*UX)
      HY=HY+SGN(I)*HG
      HZ=HZ+SGN(I)*(HH*UZ-HE*UX)
    6 IF(I-J) 20,21,21
   20 I=I+1
      GO TO 13
C  CALCULATE ANISOTROPY CONSTANTS
   21 HX=HX*UB
      HZ=HZ*UB
      IF(HAPL1) 50,50,51
   50 HX=0.0
   51 HAPL=HAPL1-16.75516*S*UB*UX*1.97525E+22
   22 DKMD=3.0*S*UB*HZ*1.97525E+22
      DKFS=1.920000E+5-DKMD
      DKXT=2.0*S*UB*(HAPL+HX)*1.97525E+22
   26 ALPHA=ABS(ALPHA)
C  CALCULATE TEMPERATURE DEPENDENCE
      HEXC=3.0*TN*BK*UZ/((S+1.0)*2.0*UB)-3.316430E+3+HZ
      B1=HEXC**2+HX*HX
      C1=2.0*HX*HAPL
   28 A1=2.0*UB*S/(BK*TI)
      X=A1*DSQRT(B1+C1+HAPL**2*1.0000)
   34 X1=((2.0*S+1.0)/(2.0*S))*X
      X2=X/(2.0*S)
      HA=1.0/DTANH(X1)
      HB=1.0/DTANH(X2)
      HC=2.0/(DEXP(X1)-DEXP(-X1))
      HD=2.0/(DEXP(X2)-DEXP(-X2))
```

```
      BX1=((4.*S*S+4.*S+1.)*HA*HA-(4.*S+2.)*HA*HB+HB*HB)/(4.*S*S)
     0BX=BX1-(-C1/(2.*B1)+DSQRT((C1/(2.*B1))**2+(X**2-(A1*HAPL)**2)/
     1(A1*A1*B1)))**2
      IF(BX) 32,35,31
   31 TI=TI/1.01
      PRINT 37,TN
      GO TO 28
  320DBX=HA*HD*HD*(2.0*S+1.0)/(4.0*S**3)-HA*HC*HC*2.*((2.0*S+1.)/
     1(2.0*S))**3+HB*HC*HC*(2.0*S+1.0)**2/(4.0*S**3)-2.0*HB*HD*HD/
     2(2.*S)**3-2.*(-C1/(2.*B1)+DSQRT((C1/(2.*B1))**2
     2+(X**2-(A1*HAPL)**2)/
     3(A1*A1*B1)))*(X/(A1*A1*B1*DSQRT((C1/(2.*B1))**2
     4+(X**2-(A1*HAPL)**2)/(A1*A1*B1))))
      IF(DABS(BX)-1.0D-4) 35,35,33
   33 X=X-(BX/DBX)
      GO TO 34
   35 BS2=BX1
      BS=SQRT(BS2)
      BFS=(S/(S-0.5))*((S+1.0)/S-3.0*BS*HB/(2.0*S))
      DK=(DKFS*BFS+DKMD*BS2)*UZ-DKXT*BS*UX
      EXC=HEXC
      TORK=ABS(UX)*EXC-UZ*(HAPL/BS+HX)
      IF(TORK) 27,29,42
   27 IF(ABS(TORK)-0.5) 29,29,41
   41 SPERP=UB*S*(S+1.)*(HAPL+HX)*UZ/(3.*BK*TN)
     0SPARA=UB*S*(S+1.)*2.*(HAPL+HX)*ABS(UX)/(3.*BK*TN*(1.+(S+1.)*TI/
     1(3.0*S*TN*BS)))
      ALP=ALPHA
      ALPHA=ALPHA+ATAN(SPERP/(S+SPARA))/CVEX
      GO TO 12
   42 IF(ABS(TORK)-0.5) 29,29,52
   52 ALPHA=ALP
      CVEX=CVEX*10.0
      GO TO 12
   29 TNORM=TI/TN
      PRINT 37,DK,ALPHA,HAPL1,TI,TNORM
      IF(DK) 44,60,60
   60 IF(TI-TH) 36,44,44
   36 TI=TI+DT
      GO TO 45
   44 PRINT 46
      GO TO 43
   23 FORMAT(5E14.7,F5.1,I5)
   24 FORMAT(E14.7,F5.1,E14.7)
   25 FORMAT(F5.1,I5)
   37 FORMAT(5E16.7)
   46 FORMAT(//)
   47 CALL EXIT
      END
```

```
MACHINE PROGRAM FOR CALCULATION OF THE DIPOLAR FIELDS
   DIMENSION RX(600),RY(600),RZ(600),R(600),R3(600),SGN(600)
   DIMENSION UBX(21),NI(21),N(600)
 1 I=1
READ - ION LOCATION AND SPIN SIGN FOR N IONS
 2 READ 23,RX(I),RY(I),RZ(I),R(I),R3(I),SGN(I),N(I)
   IF(RX(I)-1.0) 4,8,4
 4 I=I+1
   GO TO 2
 8 J=I-1
READ - BOHR MAGNETON, UB PER DIPOLE, 1.0E-24
   READ 24,UB,UBN,RRR
   I=1
READ - UB PER IMPURITY ION, IMPURITY ION NUMBER
 9 READ 25,UBX(I),NI(I)
   IF(UBX(I)-99.0) 10,11,11
10 I=I+1
   GO TO 9
11 NIMP=I-1
READ - SUBLATTICE (-1.0,0.0,OR 1.0)
   READ 25,SUB
READ - ROTATION INCREMENT, ROTATION LIMIT
   READ 23,DPHI,HPHI
READ - CANTING ANGLE ALPHA
22 READ 23,ALPHA
   IF(ALPHA) 34,26,26
26 UX=SINF(ALPHA)
   UZ=COSF(ALPHA)
36 PHI=0.0
12 HX=0.0
   HY=0.0
   HZ=0.0
   PS=SIN(PHI)
   PC=COS(PHI)
   I=2
13 IF(SGN(I)-SUB) 5,6,5
 5 ALPHA=ABSF(ALPHA)*SGN(I)
   UX=ABS(UX)*SGN(I)
LATTICE ROTATION MATRIX, NEXT 3 CARDS
   RX1=RX(I)*PC-RZ(I)*PS
   RY1=RY(I)
   RZ1=RX(I)*PS+RZ(I)*PC
   AA=(ABS(UX)*(RX1- RX(1))+UZ*SGN(I)*(RZ1-RZ(1)))/R(I)
   IF(AA**2-1.0)3,3,7
 7 AA=1.0
 3 BB=SQRT(1.0-AA**2)
   X3=(RX1-RX(1))*UZ-(RZ1-RZ(1))*UX
```

```
      R1=SQRT(X3**2+(RY1-RY(1))**2)
      IF(R1) 15,14,15
   14 CC=0.0
      DD=0.0
      GO TO 16
   15 CC=X3/R1
      DD=(RY1-RY(1))/R1
   16 HF=3.0*AA*BB*CC/R3(I)
      HG=3.0*AA*BB*DD/R3(I)
      HH=(3.0*AA**2-1.0)/R3(I)
      DO 18 K=1,NIMP
      IF(N(I)-NI(K)) 18,17,18
   17 HE=HE*UBX(K)/RRR
      HG=HG*UBX(K)/RRR
      HH=HH*UBX(K)/RRR
      GO TO 19
   18 CONTINUE
      HE=HE*UBN/RRR
      HG=HG*UBN/RRR
      HH=HH*UBN/RRR
   19 HX=HX+SGN(I)*(HE*UZ+HH*UX)
      HY=HY+SGN(I)*HG
      HZ=HZ+SGN(I)*(HH*UZ-HE*UX)
    6 IF(I-J) 20,21,21
   20 I=I+1
      GO TO 13
   21 HX=HX*UB
      HY=HY*UB
      HZ=HZ*UB
      PRINT 37,HX,HY,HZ,ALPHA,PHI
      IF(PHI-HPHI)27,22,22
   27 PHI=PHI+DPHI
      GO TO 12
   23 FORMAT(5E14.7,F5.1,I5)
   24 FORMAT(E14.7,F5.1,E14.7)
   25 FORMAT(F5.1,I5)
   37 FORMAT(6E16.7)
   34 CALL EXIT
      END
```

```
MACHINE PROGRAM FOR SOLUTION OF BRILLOUIN FUNCTION
   DOUBLE PRECISION  X1,X2,HA,HB,HC,HD,BX,DBX,X
    DOUBLE PRECISION A1,B1,C1,HEXC,BX1
READ - NEEL TEMP, TEMP INCREMENT, INITIAL TEMP, FINAL TEMP
43 READ 23,TN,DT,TI,TH
    IF(TN) 5,5,6
READ - EXTERNAL FIELD PERPENDICULAR TO SPIN
 6 READ 23,HAPL
READ - SPIN QN, BOLTZMANN CONSTANT
    READ 23,S,BK
READ INDUCED DIPOLAR FIELDS
    READ 23,HX,HZ
    PRINT 26, HX,HZ,HAPL
    HEXC=3.0*TN*BK/((S+1.0)*2.0*UB)+HZ
    B1=HEXC**2+HX*HX
    C1=2.0*HX*HAPL
28 A1=2.0*UB*S/(BK*TI)
    X=A1*DSQRT(B1+C1+HAPL**2*1.0D00)
34 X1=((2.0*S+1.0)/(2.0*S))*X
    X2=X/(2.0*S)
    HA=1.0/DTANH(X1)
    HB=1.0/DTANH(X2)
    HC=2.0/(DEXP(X1)-DEXP(-X1))
    HD=2.0/(DEXP(X2)-DEXP(-X2))
    BX1=((4.*S*S+4.*S+1.)*HA*HA-(4.*S+2.)*HA*HB+HB*HB)/(4.*S*S)
  DBX=BX1-(-C1/(2.*B1)+DSQRT((C1/(2.*B1))**2+(X**2-(A1*HAPL)**2)/
  1(A1*A1*B1)))**2
320DBX=HA*HD*HD*(2.0*S+1.0)/(4.0*S**3)-HA*HC*HC*2.*((2.0*S+1.)/
  1(2.0*S))**3+HB*HC*HC*(2.0*S+1.0)**2/(4.0*S**3)-2.0*HB*HD*HD/
  2(2.*S)**3-2.*(-C1/(2.*B1)+DSQRT((C1/(2.*B1))**2
  2+(X**2-(A1*HAPL)**2)/
  3(A1*A1*B1)))*(X/(A1*A1*B1*DSQRT((C1/(2.*B1))**2
  4+(X**2-(A1*HAPL)**2)/(A1*A1*B1))))
    IF(DABS(BX)-1.0D-4) 35,35,33
33 X=X-(BX/DBX)
    GO TO 34
35 BS2=BX1
    BS=SQRT(BS2)
    BFS=(S/(S-0.5))*((S+1.0)/S-3.0*BS*HB/(2.0*S))
    TNORM=TI/TN
    PRINT 37,BS2,BS,BFS,TI,TNORM
    IF(TI-TH) 4,43,43
 4 TI=TI+DT
    GO TO 28
23 FORMAT(4E14.7)
26 FORMAT(5X,3E16.7/)
37 FORMAT(6E16.7)
 5 CALL EXIT
    END
```

# LITERATURE CITED

1. L. Néel, Ann. Phys. (Paris) 17, 64(1932).

2. F. J. Morin, Phys. Rev. 78, 819(1950).

3. J. O. Artman, J. C. Murphy, S. Foner, Phys. Rev. 138, A912(1965).

4. J. Kanamori, Magnetism Vol. I, edited by G. Rado and H. Suhl (Academic Press, 1963), pp. 172-3.

5. I. Dzyaloshinski, J. Phys. Chem. Solids 4, 241(1958).

6. T. Moriya, Magnetism Vol. I, edited by G. Rado and H. Suhl (Academic Press, 1963) Ch. 3, and T. Moriya, Phys. Rev. 120, 91(1960).

7. L. Néel, R. Panthenet, C. R. Acad. Sci., Paris, 234, 2172(1952).

8. C. Ransom, Data recorded at MSU.

9. M. Tachiki and T. Nagamiya, J. Phys. Soc. Japan 13, 452(1958).

10. K. Yosida, Progr. Theor. Phys. 6, 691(1951).

11. S. T. Lin, Phys. Rev. 116, 1447(1959).

12. R. E. Newnham and Y. M. deHaan, Zeit. Krist. 117, S235(1962).

13. A. H. Morrish, The Physical Principles of Magnetism (Wiley, 1965), Ch. 6.

14. J. Kanamori, Magnetism Vol. I, edited by G. Rado and H. Suhl (Academic Press, 1963), pp. 144-159.

15. J. H. Van Vleck, J. Chem. Phys. 9, 85(1941).